

# A Study of Specific Heat Capacity Functions of Polyvinyl Alcohol–Cassava Starch Blends

Lee Tin Sin · W. A. W. A. Rahman ·  
A. R. Rahmat · N. A. Morad · M. S. N. Salleh

Received: 30 September 2009 / Accepted: 19 April 2010 / Published online: 8 May 2010  
© Springer Science+Business Media, LLC 2010

**Abstract** The specific heat capacity ( $C_{sp}$ ) of polyvinyl alcohol (PVOH) blends with cassava starch (CSS) was studied by the differential scanning calorimetry method. Specimens of PVOH–CSS blends: PPV37 (70 mass% CSS) and PPV46 (60 mass% CSS) were prepared by a melt blending method with glycerol added as a plasticizer. The results showed that the specific heat capacity of PPV37 and PPV46 at temperatures from 330 K to 530 K increased from (2.963 to 14.995)  $J \cdot g^{-1} \cdot K^{-1}$  and (2.517 to 14.727)  $J \cdot g^{-1} \cdot K^{-1}$ , respectively. The specific heat capacity of PVOH–CSS depends on the amount of starch. The specific heat capacity of the specimens can be approximated by polynomial equations with a curve fitting regression  $>0.992$ . For instance, the specific heat capacity (in  $J \cdot g^{-1} \cdot K^{-1}$ ) of PPV37 can be expressed by  $C_{sp} = -17.824 + 0.063T$  and PPV46 by  $C_{sp} = -18.047 + 0.061T$ , where  $T$  is the temperature (in K).

**Keywords** Cassava starch · Polyvinyl alcohol · Specific heat capacity

## 1 Introduction

Biodegradable polymeric materials have gained the attention of researchers in recent years. Biodegradable polymers such as polyvinyl alcohol (PVOH) [1], polylactic acid [2], polycaprolactone [3], polyanhydrides [4], etc. have been expected to bring many

L. T. Sin (✉) · W. A. W. A. Rahman · A. R. Rahmat · M. S. N. Salleh  
Department of Polymer Engineering, Faculty of Chemical and Natural Resources Engineering,  
Universiti Teknologi Malaysia, 81310 Skudai, Johor, Malaysia  
e-mail: direct.tinsin@gmail.com

N. A. Morad  
Department of Mechanical Engineering, College of Science and Technology, Universiti Teknologi  
Malaysia, International Campus, Jalan Semarak, 54100 Kuala Lumpur, Malaysia

benefits to mankind. However, the prices of such synthetic biodegradable polymers are expensive with limited amounts being produced worldwide annually. Thus, blending of synthetic biodegradable polymers with other natural bio-polymers- i.e., starch or cellulose is considered as a feasible approach to produce economical products [5]. Starch or cellulose is a naturally occurring bio-polymer. Starch is available abundantly at a cheap price. The applications of biodegradable starch polymeric materials are recognized worldwide. To name some, a biodegradable starch bio-material is suitable to substitute for a petroleum-based packaging material. It can help to reduce overloading of non-degradable plastic solid wastes in landfills. Biodegradable starch biomaterials are readily consumed by microbes after exposure to the natural environment [6]. Besides that, starch-based biopolymers have been widely used in the biomedical industry as tissue scaffolding material [7]. Biodegradable polymers promote growth of cells and will degrade after formation of tissues [8].

The goal of this work is to investigate the specific heat capacity ( $C_{sp}$ ) of PVOH–cassava starch (CSS) blends and its dependence on temperature.  $C_{sp}$  can be represented by  $\Delta Q/(m\Delta T)$ , where  $\Delta Q$ ,  $m$ , and  $\Delta T$  are the change of heat, mass, and change of temperature, respectively.  $C_{sp}$  plays an important role to reflect the molecular structure of substances [9, 10]. It is also an important property for product performance and process engineering [9, 11]. Fujino and Honda [11] have measured the  $C_{sp}$  of plastic waste/fly ash (PWFA) composite materials for cable troughs shielding underground lines. The study has provided important information about the ability of PWFA insulation material to dissipate generated heat due to electrical resistance. Similarly, PVOH–starch has the potential in food packaging applications. Measurements of  $C_{sp}$  of PVOH–starch help to determine the ability of PVOH–starch to keep the food in a warm condition. In addition,  $C_{sp}$  can also be used to predict heat removal during the cooling stage in an injection molding process [12]. Stable heat removal is important to avoid occurrence of severe warpage and internal stress, which will degrade product performance.

Several researchers have conducted a study of  $C_{sp}$  of neat PVOH and starches from various origins. For instance, Pyda and coworkers [9, 13] have developed a database known as ATHAS (The Advanced Thermal Analysis System) for a wide range of polymer materials including PVOH, which is available on the internet [14]. A similar  $C_{sp}$  of PVOH was adopted by Wen [15], for which  $C_{sp}$  of PVOH is  $1.185 \text{ kJ} \cdot \text{kg}^{-1} \cdot \text{K}^{-1}$  and  $1.546 \text{ kJ} \cdot \text{kg}^{-1} \cdot \text{K}^{-1}$  at  $250 \text{ K}$  and  $300 \text{ K}$ , respectively. On the other hand, Louder et al. [16] have published works on  $C_{sp}$  of starches from different origins. The results show that native starches from various sources (maize, potato, and wheat) have remarkably different values of  $C_{sp}$ . One of the main factors that caused the differences was due to the variation of moisture content in the starches. Water has a higher  $C_{sp}$  as compared to pure starch. When the starches were dehydrated, the  $C_{sp}$  of potato and wheat starches approached each other. However, the  $C_{sp}$  of maize starch still remained higher than for potato and wheat starches. This indicates that even though starches originally are built up of the D-glucose unit, differences in compositions of amylose and amylopectin resulted in variations in  $C_{sp}$  [17]. Besides that, Tan et al. [18] have studied the  $C_{sp}$  of thermoplastic starch with different amounts of plasticizers (water and glycerol) added. The results showed that  $C_{sp}$  increased proportionally with the water content. Glycerol content in thermoplastic starch influenced the thermal property according to starch

types. Thus, it can be postulated that  $C_{sp}$  is able to provide remarkable “fingerprints” to distinguish properties of various polymers blends.

## 2 Experimental

### 2.1 Materials

Fully hydrolyzed PVOH grade BF-17H (viscosity of (0.025 to 0.030) Pa·s, hydrolysis (99.4 to 99.8) mol%, ash < 0.7 %) manufactured by Chang Chung Petrochemical Co., Ltd. was used. Native CSS was obtained from Thailand-Cap Kapal ABC. Glycerol ( $C_3H_8O_3$ ) at 99.5 % purity was purchased from Fisher Scientific. Calcium stearate (CaS) was supplied by Sun Ace Kakoh (M) Sdn. Bhd. Phosphoric acid at 85 % purity was obtained from Merck. CaS and phosphoric acid were used as an internal lubricant and heat stabilizer additive, respectively. All these materials were used as received.

### 2.2 Specimen Preparation

PVOH, glycerol, CaS, and phosphoric acid were pre-mixed in a Chyau Long Machinery Co., Ltd. CL-10 high-speed mixer for 15 min. After that, the mixtures were compounded using a twin screw co-rotating extruder Sino PSM 30 B5B25 (built by Sino-Alloy Machinery Inc.) to produce plasticized PVOH (PPVOH). The composition of PPVOH is shown in Table 1. A side feeder was used to transfer the mixtures into a barrel with four heating zones. All heating zones were set to 160 °C while the screw speed was set to 250 rpm. After that, PPVOH, CSS, and glycerol were mixed again in a high-speed mixer as PPVOH–CSS mixtures with compositions as shown in Table 2. The mixtures were compounded again in a similar twin screw co-rotating extruder. Four heating zones were set at 140 °C while the screw speed was set at 250 rpm. The extruded compounds were palletized and immediately sealed in polyethylene bags.

**Table 1** Composition of plasticized PVOH (PPVOH)

Specimen	Glycerol (phr)	PVOH (phr)	CaS (phr)	Phosphoric acid (g)
PPVOH	40	100	2	4.18

**Table 2** Composition of PPVOH–CSS blends

Specimen	PPVOH (mass%)	CSS (mass%)	Glycerol (phr)
PPV37	30	70	20
PPV46	40	60	20

### 2.3 Experimental Specific Heat Capacity ( $C_{sp}$ ) Measurements

$C_{sp}$  of specimens was measured by differential scanning calorimetry (DSC)—Perkin Elmer DSC7. A synthetic sapphire disc was used as the reference material. The estimated overall uncertainty of the specific heat capacity measurements is 10 %. The measurements were conducted in the temperature range from 330 K to 530 K at a scanning rate of  $10\text{ }^{\circ}\text{C} \cdot \text{min}^{-1}$  with nitrogen purging at  $20\text{mL} \cdot \text{min}^{-1}$ . Sealed aluminum pans were used to encapsulate specimens or sapphire for measurements. The procedure to determine  $C_{sp}$  data was based on three DSC runs.

1. Measurement of empty aluminum pan.
2. Measurement of sapphire (mass 9.8 mg) as the reference material. The standard sapphire specific heat capacity data were extracted from BS ISO 11357-4 [19] and tabulated in Table 3.
3. Measurement of specimens (mass of 9 mg to 15 mg).

Each specimen was tested in duplicate to ensure reproducibility of the results. The specific heat capacity of the specimen,  $C_{sp}$  is given by

$$C_{sp} = \frac{M_{rs}}{M_{sp}} \times \frac{\Delta S_{sp}}{\Delta S_{rs}} \times C_{rs} \quad (1)$$

where  $C_{rs}$  is the known specific heat capacity of the sapphire standard reference material.  $M_{rs}$  and  $M_{sp}$  are the masses of the sapphire reference material and specimen, respectively.  $\Delta S_{rs}$  is the signal difference between the sapphire reference material and empty aluminum pan, and  $\Delta S_{sp}$  is the signal difference between the specimen and empty aluminum pan.

**Table 3** Tabulated specific heat capacity of sapphire reference material and specimens

Temperature (K)	Specific heat capacity $C_{sp}$ ( $\text{J} \cdot \text{g}^{-1} \cdot \text{K}^{-1}$ )			Temperature (K)	Specific heat capacity $C_{sp}$ ( $\text{J} \cdot \text{g}^{-1} \cdot \text{K}^{-1}$ )		
	Sapphire <sup>a</sup>	PPV37	PPV46		Sapphire <sup>a</sup>	PPV37	PPV46
330	0.837	2.963	2.517	440	0.988	10.273	8.624
340	0.855	3.481	2.942	450	0.998	11.016	9.448
350	0.871	4.035	3.395	460	1.007	11.493	9.698
360	0.887	4.632	3.890	470	1.016	11.929	10.020
370	0.902	5.268	4.420	480	1.025	12.189	10.366
380	0.916	5.928	4.977	490	1.033	13.068	11.577
390	0.930	6.595	5.550	500	1.041	13.523	12.565
400	0.942	7.292	6.141	510	1.048	14.139	13.376
410	0.954	7.999	6.752	520	1.056	14.746	14.127
420	0.966	8.729	7.337	530	1.063	14.995	14.727
430	0.977	9.468	7.943				

Variations of the above data are within  $\pm 10\%$

<sup>a</sup> Reference material

### 3 Results and Discussion

Figure 1 shows DSC thermograms of the empty aluminum pan, sapphire, PPV37, and PPV46. These are the basic data used to calculate  $C_{sp}$ . The results for PPV37 and PPV46 are tabulated in Table 3. These data are further plotted in Fig. 2. As noticed,  $C_{sp}$  of both specimens PPV37 and PPV46 increased monotonically with temperature. However, there were still small increments of  $C_{sp}$  in the melting range of 440 K to 480 K. PPV46 has a higher amplitude increment of  $C_{sp}$  in the melting range compared to PPV37. It was because PPV46 contains higher amounts of PVOH than does

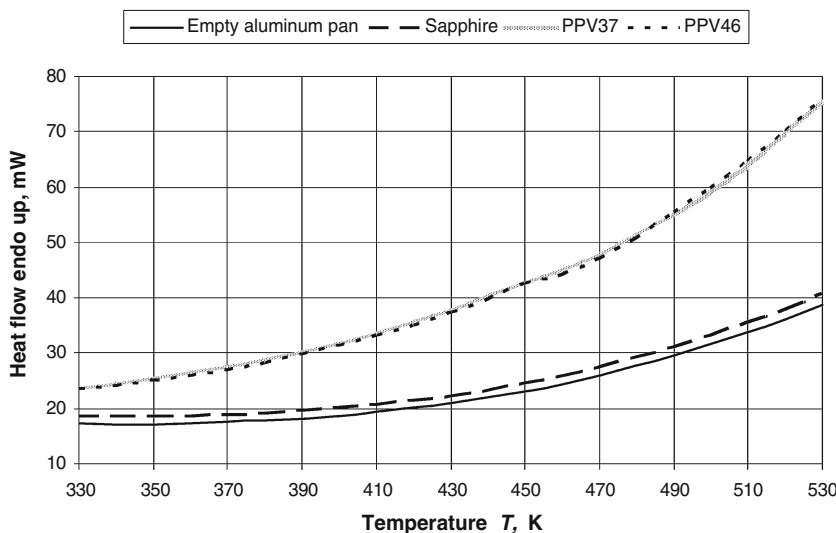


**Fig. 1** DSC thermograms of empty aluminum pan, sapphire, PPV37, and PPV46

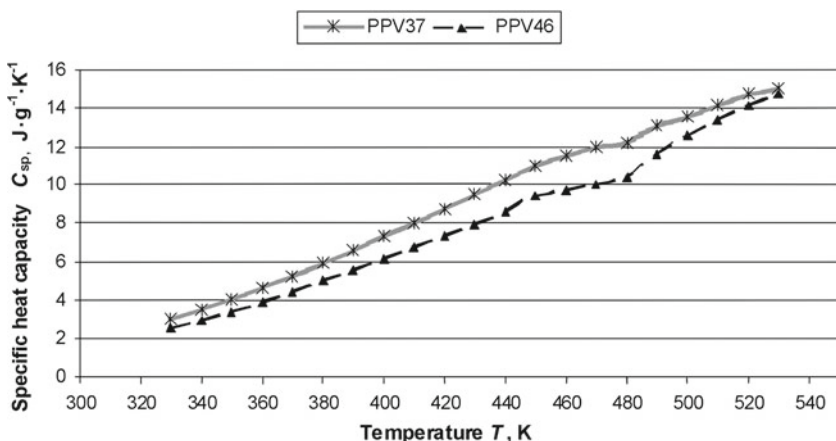


**Fig. 2** Specific heat capacity ( $C_{sp}$ ) of PPV37 and PPV46 specimens

PPV37. PPV46 required extra energy to achieve the melting stage [5]. The enthalpy of melting played a role to produce a higher  $C_{sp}$ . Besides that, PPV37 has an overall  $C_{sp}$  higher than that of PPV46. This was due to PPV37 containing a higher amount of CSS and it possessed a lower rigidity than PPV46. A higher rigidity limits the molecular structure to mere vibrational motion when subjected to thermal effects. Whereas a lower rigidity molecule system such as those found in amorphous or liquid states would induce a number of skeletal vibrations, changes in conformational character and large-amplitude motion caused anharmonic interactions when subjected to a thermal effect. Subsequently, this would contribute a significant higher  $C_{sp}$  [13].

The experimental data have been correlated with five different equations in describing  $C_{sp}$  as a function of temperature. Since  $C_{sp}$  of both PPV37 and PPV46 increased monotonically with temperature and did not show substantial changes of  $C_{sp}$  during the melting state, polynomial equations are adequate to represent the relationship.

1. Linear or first-order polynomial:

$$C_{sp} = C_1 + C_2 T \quad (2)$$

2. Cubic or third-order polynomial:

$$C_{sp} = C_1 + C_2 T + C_3 T^2 + C_4 T^3 \quad (3)$$

3. Form proposed by Chen et al. [20]:

$$C_{sp} = C_1 + C_2 T + C_3 T^{-2} \quad (4)$$

4. Form proposed by Itagaki and Yamaguchi [21]:

$$C_{sp} = C_1 + C_2 T + C_3 T^{-2} + C_4 T^2 \quad (5)$$

5. Form proposed by Leitner et al. [22,23]:

$$C_{sp} = C_1 + C_2 T + C_3 T^{-2} + C_4 T^{-3} \quad (6)$$

where  $C_{sp}$  is the specific heat capacity (in  $\text{J} \cdot \text{g}^{-1} \cdot \text{K}^{-1}$ );  $T$  is the temperature (in K); and  $C_1$ ,  $C_2$ ,  $C_3$ , and  $C_4$  are adjustable parameters. The adjustable parameters were predicted by a non-linear regression method using the SPSS 16 statistical package. The results of the adjusted parameters and curve fitting regression of the equations are shown in Table 4. All equations have shown good fits for both PPV37 and PPV46 curves. However, among the five equations, the best results of PPV37 correlations have been obtained for the third-order polynomial (cubic) and Itagaki and Yamaguchi [21] equations. Meanwhile, the third-order polynomial (cubic), Itagaki and Yamaguchi [21], and Leitner et al. [22,23] equations have shown the highest regression to fit the PPV46 curves. The comparisons of the best fit equations corresponding to experimental results are shown in Figs. 3 and 4 for PPV37 and PPV46, respectively.

**Table 4** Results of adjusted parameters and curve fitting regressions of equations

Specimen	Coefficient	Linear First order	Cubic Third order	Chen et al. [20]	Itagaki and Yamaguchi [21]	Leitner et al. [22]
PPV37	$C_1$	−17.824	30.011	−10.689	−26.398	−14.758
	$C_2$	0.063	−0.300	0.052	0.104	0.058
	$C_3$	—	$9.030 \times 10^{-4}$	−410297	1.010	−176248
	$C_4$	—	$−7.357 \times 10^{-7}$	—	$−4.731 \times 10^{-5}$	22855
Regression		0.996	0.999	0.997	0.998	0.997
PPV46	$C_1$	−18.047	−34.996	−18.801	−4.246	−66.866
	$C_2$	0.061	0.215	0.062	−0.005	0.123
	$C_3$	—	$−4.4 \times 10^{-4}$	42770	1.017	6965759
	$C_4$	—	$4.010 \times 10^{-7}$	—	$7.615 \times 10^{-5}$	$−1.272 \times 10^9$
Regression		0.992	0.997	0.993	0.997	0.997

Although the first-order polynomial equation showed the lowest regression for both PPV37 and PPV46 curves, the linear equation remains the simplest and most widely proposed equation to represent the relationship of the specific heat capacity and temperature [11, 24]. The reason the linear equation has the lowest regression for PPV37 and PPV46 is mainly due to deviations in the melting states from 440 K to 480 K. The highest percentage errors of the first-order polynomial equation predictions for PPV37 (at 450 K) and PPV46 (at 480 K) were 4.45 % and 8.36 %, respectively. Consequently, the deviations of the predicted values using the first-order polynomial equation from experimental results in the melting range from 440 K to 480 K are still considered to be acceptable.

#### 4 Conclusions

Measurements of the specific heat capacity of PVOH–CSS blends were conducted with the DSC method. The following findings were obtained.

- (1)  $C_{sp}$  of PVOH–CSS for the temperature range from 330 K to 530 K increased from (2.963 to 14.995)  $\text{J} \cdot \text{g}^{-1} \cdot \text{K}^{-1}$  and (2.517 to 14.727)  $\text{J} \cdot \text{g}^{-1} \cdot \text{K}^{-1}$  for PPV37 and PPV46, respectively.
- (2)  $C_{sp}$  of PVOH–cassava starch depends on the amount of starch.
- (3) PPV37 and PPV46 showed small increments of  $C_{sp}$  in the melting states from 440 K to 480 K. However, the increment is significant to affect the effort to approximate  $C_{sp}$  of PPV37 and PPV46 as functions of temperature by polynomial equations with a curve fitting regression  $>0.992$ .
- (4) Although the first-order polynomial equation has the lowest curve fitting regression due to the presence of the melting state in PVOH–CSS specimens, the equation is still sufficient to represent  $C_{sp}$  of PPV37 and PPV46 with highest percentage errors of prediction of 4.45 % and 8.36 %, respectively, at the melting state.

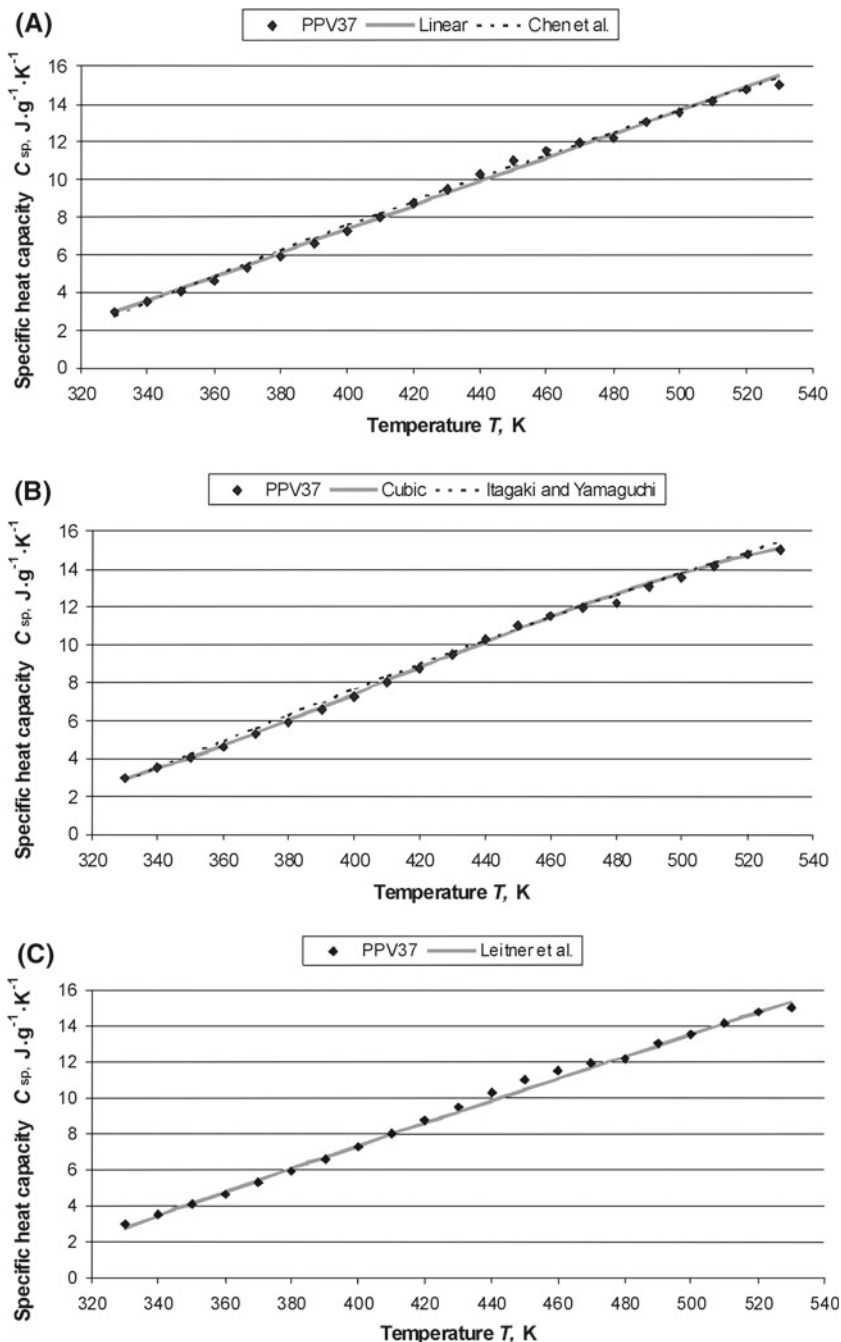


**Fig. 3** Comparisons of experimental data for PPV37 with model equations (Chen et al. [20]; Itagaki and Yamaguchi [21]; Leitner et al. [22])

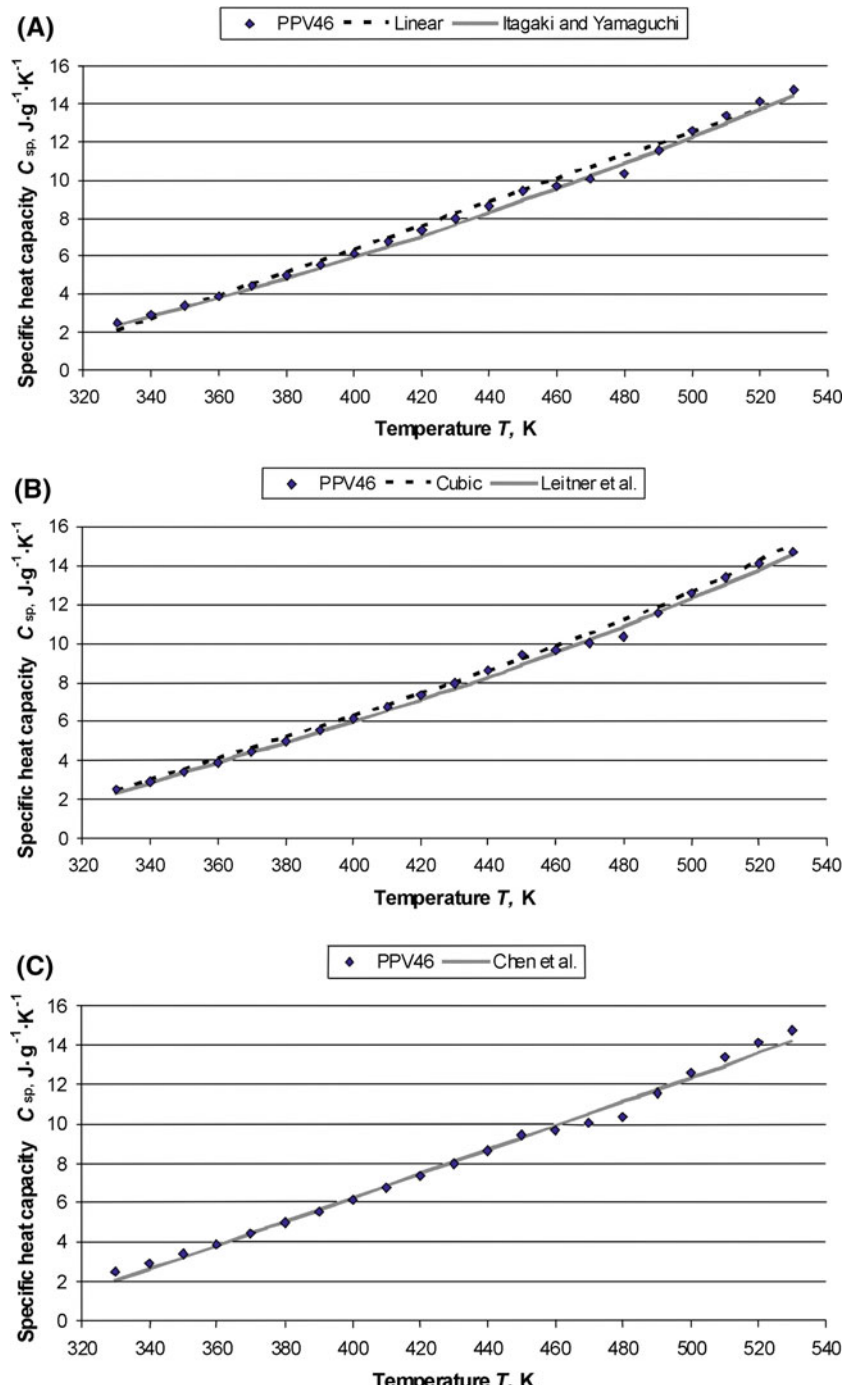


**Fig. 4** Comparisons of experimental data for PPV46 with model equations (Itagaki and Yamaguchi [21]; Leitner et al. [22]; Chen et al. [20])

**Acknowledgments** This project is supported by the Ministry of Science, Technology and Innovations (MOSTI) of The Federal Government of Malaysia-Putrajaya under eScienceFund 03-01-06-SF0468 and the National Science Fellowship 1/2008.

## References

1. E. Chiellini, A. Corti, D. Salvatore, R. Solaro, *Prog. Polym. Sci.* **28**, 963 (2003)
2. L.J. Chang, *J. Polym. Environ.* **8**, 33 (2000)
3. R. Chandra, R. Rustgi, *Prog. Polym. Sci.* **23**, 273 (1998)
4. L.S. Nair, C.T. Laurencin, *Prog. Polym. Sci.* **32**, 762 (2007)
5. L.T. Sin, W.A.W.A. Rahman, A.R. Rahmat, M.I. Khan, *Carbohydr. Polym.* **79**, 224 (2010)
6. T. Ishigaki, Y. Kawagoshi, M. Ike, M. Fujita, *World J. Microbiol. Biotechnol.* **15**, 321 (1999)
7. N.M. Neves, A. Kouyumdzhiev, R.L. Reis, *Mater. Sci. Eng. C* **25**, 195 (2005)
8. A. Sinha, G. Das, K. Sharma B., R.P. Roy, A.K. Pramanick, S. Nayar, *Mater. Sci. Eng. C* **27**, 70 (2007)
9. M. Pyda, E. Nowak-Pyda, J. Mays, B. Wunderlich, *J. Polym. Sci. B Polym. Phys.* **42**, 4401 (2004)
10. L.H. Sperling, *Introduction to Physical Polymer Science*, 4th edn. (Wiley, New Jersey, 2006), pp. 367–374
11. J. Fujino, T. Honda, *Int. J. Thermophys.* **30**, 976 (2009)
12. B. Likazor, M. Krajnc, *Chem. Eng. Sci.* **63**, 3181 (2008)
13. M. Pyda, R.C. Bopp, B. Wunderlich, *J. Chem. Thermodyn.* **36**, 731 (2004)
14. M. Pyda (ed.), ATHAS Data Bank. Available from <http://athas.prz.edu.pl/> (2009)
15. J. Wen, in *Physical Properties of Polymer Handbook*, 2nd edn., ed. by J.E. Mark (Springer, New York, 2007), p. 149
16. W. Louder, A-H. Meniai, J.-P.E. Grolier, *J. Therm. Anal. Calorim.* **93**, 605 (2008)
17. V.P. Yuryev, E.N. Kalistratova, A.N. Danilenko, V.A. Protserov, A.V. Persikov, *Starch-Stärke* **51**, 160 (1999)
18. I. Tan, C.C. Wee, P.A. Sopade, P.J. Halley, *Starch-Stärke* **56**, 6 (2004)
19. British Standard Institutions, Plastics-BS ISO 11357-4. Differential scanning calorimetry (DSC) Part 4: Determination of specific heat capacity (2005)
20. X. Chen, Y. Lan, J. Liang, X. Cheng, Y. Xu, T. Xu, P. Jiang, K. Lu, *Chin. Phys. Lett.* **16**, 107 (1999)
21. K. Itagaki, K. Yamaguchi, *Thermochim. Acta* **163**, 1 (1990)
22. J. Leitner, A. Strejc, D. Sedmidubský, K. Růžička, *Thermochim. Acta* **401**, 169 (2003)
23. I. Zięborak-Tomaszkiewicz, E. Utzig, P. Gierycz, *J. Therm. Anal. Calorim.* **91**, 329 (2008)
24. E. Marti, E. Kaisersberger, E. Moukhina, *J. Therm. Anal. Calorim.* **85**, 505 (2006)